

Quantum computing with magnetic atoms in optical lattices of reduced periodicity

Boris Ravaine,¹ Andrei Derevianko,¹ and P. R. Berman²

¹*Department of Physics, University of Nevada, Reno, Nevada 89557, USA*

²*Michigan Center for Theoretical Physics, FOCUS Center, and Department of Physics,*

University of Michigan, Ann Arbor, Michigan 48109, USA

(Received 24 June 2006; published 29 August 2006)

We investigate the feasibility of combining Raman optical lattices with a quantum computing architecture based on lattice-confined magnetically interacting neutral atoms. A particular advantage of the standing Raman field lattices comes from reduced interatomic separations leading to increased interatomic interactions and improved multiqubit gate performance. Specifically, we analyze a $J=3/2$ Zeeman system placed in σ_+ - σ_- Raman fields which exhibit $\lambda/4$ periodicity. We find that the resulting controlled-NOT (CNOT) gate operations times are in the order of millisecond. We also investigate motional and magnetic-field induced decoherences specific to the proposed architecture.

DOI: [10.1103/PhysRevA.74.022330](https://doi.org/10.1103/PhysRevA.74.022330)

PACS number(s): 03.67.Lx, 03.65.Yz, 32.80.Wr, 32.80.Qk

I. INTRODUCTION

Controlled interactions between qubits is the key to practical realization of quantum multiqubit gates. The strength of the interaction determines how fast the gate operations are performed. In Ref. [1], a quantum computing scheme based on magnetically interacting atoms held in optical lattice was proposed. Since the interaction between magnetic dipoles separated by a distance R scales as $1/R^3$, it is beneficial to reduce the distance between the atoms. In traditional optical lattices, created by two interfering counter-propagating laser fields of wavelength λ , the interatomic distance is $\lambda/2$. The estimates [1] show that a resulting controlled-NOT (CNOT)-gate performance time τ_{CNOT} ranges from 10^{-2} s for alkalis to 10^{-4} s for complex open-shell atoms with large magnetic moments, such as dysprosium.

Recently optical lattices of reduced, $\lambda/2^n$ ($n=1, 2, 3, \dots$), periodicity have been proposed [2,3] and are under experimental investigation [4]. Here we evaluate a feasibility of combining such lattices with the quantum computing scheme of Ref. [1]. Compared to the conventional $\lambda/2$ lattices, such a combination could potentially yield a factor of $2^{3(n-1)}$ improvement in the gate performance time. In this paper we analyze the case of a $\lambda/4$ lattice.

The paper is organized as follows. In Sec. II, we review the relevant features of the quantum computing architecture with magnetic atoms [1]. In Sec. III, we derive optical potentials for a particular case of $J=3/2$ atoms and demonstrate their $\lambda/4$ periodicity. In Sec. IV, we describe operation of our proposed quantum computing scheme. Finally, in Sec. IV we address important issues of motional and magnetic-noise induced decoherences.

II. QUANTUM COMPUTING WITH MAGNETIC ATOMS

In Ref. [1], a scalable quantum computing architecture was proposed. The architecture utilizes magnetic interaction of complex open-shell atoms confined to the nodes of an optical lattice. The lattice is placed in a high gradient magnetic field and the resultant Zeeman sublevels define qubit states. Microwave pulses tuned to space-dependent resonant

frequencies are used for individual addressing. Nearest-neighbor magnetic-dipolar atomic interactions allow for the implementation of a quantum controlled-NOT gate. For certain atoms, the resulting single-qubit gate operation times are on the order of microseconds, while the two-qubit operations require milliseconds. These times are much faster than the anticipated decoherence times.

While the magnetic interaction is weak (so the gate operations are relatively slow), it is the goal of this paper to investigate a potential route to strengthening interatomic interactions by bringing atoms closer in optical lattices of reduced periodicity. The proposed architecture offers several distinct advantages. For example, compared to the popular scheme with Rydberg gates [5], the advantages are (i) individual addressing of atoms with *unfocused* beams of microwave radiation, (ii) coherent “always-on” magnetic-dipolar interactions between the atoms, and (iii) substantial decoupling of the motional and inner degrees of freedom.

Before proceeding further, it is worth remembering the following order-of-magnitude values relevant to the architecture of Ref. [1]: light-shifts and the depth of the optical wells are about 1 MHz, typical Zeeman splittings are 1 GHz, and the difference in the resonant Zeeman frequency for two neighboring wells is about 1 kHz.

III. OPTICAL LATTICES OF REDUCED PERIODICITY

Optical lattices of reduced periodicity have been proposed in Refs. [2,3]. In this section we review the underlying laser field-atom configuration and formalism, and then specialize the general formalism of Ref. [3] to the $J=3/2$ atomic Zeeman manifold.

In the atom-field geometry of Ref. [3], a neutral atom interacts with four laser beams of equal intensities arranged as two counter-propagating Raman pairs, see Fig. 1. The carrier frequencies of the pairs are denoted as $(\Omega_1$ and $\Omega_2)$ and $(\Omega'_1$ and $\Omega'_2)$. The lasers are off-resonant with the upper manifold H ; neglecting a small difference in detunings from the H state for the two pairs, we use a single value for the detuning Δ , although it is this difference in detuning that allows us to neglect interference (modulated Stark shifts) be-

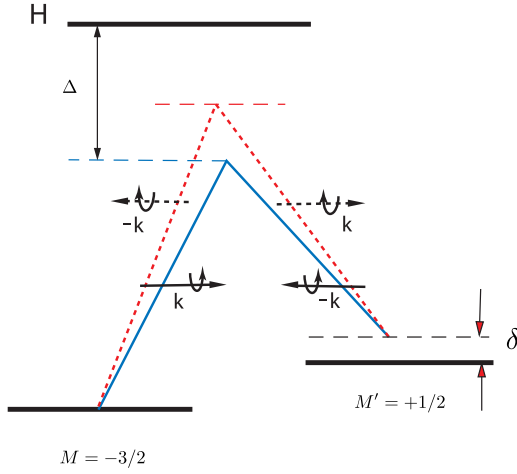


FIG. 1. (Color online) The standing wave Raman atom-field configuration is composed of four laser fields. For $J_g=3/2$ the optically coupled states are either $M=-3/2, 1/2$ or $M=-1/2, 3/2$ and the lower-manifold splitting is due to the Zeeman interaction.

tween fields having frequencies Ω_1 and Ω'_1 (or Ω_2 and Ω'_2) that would give rise to the conventional $\lambda/2$ periodicity of the optical lattice [6,7]. Each pair drives a two-photon transition between the substates g and g' of the ground-state manifold. As shown in the figure, the complementary fields Ω'_i of each pair could be detuned from resonance by $\delta = \Omega'_i - \Omega_i - \omega_{M'M}$, where $\omega_{M'M}$ is the splitting between the ground-state sublevels. In addition to Raman-induced interactions each sublevel experiences position-independent light shifts due to the interaction with the four individual laser fields.

We are interested in solving the Schrödinger equation for the described Raman atom-field geometry. At first we neglect atomic center-of-mass (c.m.) motion and obtain solutions with the optical Hamiltonian H_{opt} which incorporates internal atomic Hamiltonian and the four atom-laser interactions. We will return to the question of c.m. motion in Sec. IV. Solving the time-dependent Schrödinger equation,

$$i \frac{\partial}{\partial t} \tilde{\phi}(\xi, z, t) = H_{\text{opt}}(\xi, z, t) \tilde{\phi}(\xi, z, t), \quad (1)$$

provides dressed atomic states $\tilde{\phi}(\xi, z, t)$, where ξ and z encapsulate internal and external (c.m.) degrees of freedom, respectively. Below we outline a method of solving the above equation developed in Ref. [3]. To solve Eq. (1), we adiabatically eliminate the excited state and expand the dressed states $\tilde{\phi}(\xi, z, t)$ in terms of atomic stationary states of the lower manifold. As a result one arrives at a system of first-order linear differential equations for the amplitudes of the ground-state manifold. The right-hand side of the equations can be expressed as a matrix multiplied by a vector of ground manifold amplitudes. We denote this matrix W , it is easily reconstructed from explicit expressions given by Eq. (17) of Ref. [3]. Diagonalization of the matrix W produces a set of position-dependent optical potentials $U_i(z)$ and eigenvectors that define the dressed states $\tilde{\phi}_i(\xi, z, t)$. In Sec. III, we define qubit states in terms of these dressed states. Each

dressed state has a characteristic time dependence

$$\tilde{\phi}_i(\xi, z, t) = \phi_i(\xi, z, t) e^{-iU_i(z)t}, \quad (2)$$

the position-dependent phase leading to an optical force $-\nabla U_i(z)$ acting on the atom.

Having reviewed the general standing-wave Raman setup and the accompanying formalism, we specialize our discussion to an atom with the total angular momenta of $J_g=3/2$ for the lower manifold and $J_h=5/2$ for the upper manifold. A practically relevant example is the metastable $3p_{3/2}$ state of Al atom. It has been used in a matter-wave deposition experiment [8], where the atoms were cooled on the closed transition to the $3d_{5/2}$ state ($\lambda=309$ nm). We estimate the lifetime of the $3p_{3/2}$ state to be in the order of 10^4 seconds, much longer than the anticipated decoherence-loading-cooling time scales. A number of other open-shell atoms have $J=3/2$ ground states as well.

In the B field required for addressing individual atoms, the $J=3/2$ manifold splits into four Zeeman levels. For Al, the Lande factor is $4/3$ and the Zeeman ladder in the B field, B_0 , is given by

$$E_M = \frac{4}{3} \mu_B B_0 M.$$

The $\sigma^+ - \sigma^-$ Raman fields couple only $M=-3/2$ to $M=1/2$ and $M=-1/2$ to $M=3/2$ and effectively we deal with a pair of independent two-level subsystems. Moreover, while constructing the matrices W , we find that they are equivalent; the only difference between the subsystems comes from the fact that in the B field the level $M=-3/2$ is below $M=1/2$, while $M=3/2$ is above $M=1/2$. For zero Raman detuning δ this symmetry leads to identical optical potentials for the two subsystems. For nonzero detunings, the potentials are related to each other by changing $\delta \rightarrow -\delta$. The resulting *four* optical potentials may be parametrized as

$$U_{\pm}^{-3/2, 1/2}(z) = -\frac{\alpha}{3} \pm \frac{1}{30} \sqrt{(\alpha + 15\delta)^2 + 3\alpha^2 \cos^2(2kz)},$$

$$U_{\pm}^{3/2, -1/2}(z) = -\frac{\alpha}{3} \pm \frac{1}{30} \sqrt{(\alpha - 15\delta)^2 + 3\alpha^2 \cos^2(2kz)}, \quad (3)$$

where the superscripts in $U_{\pm}^{M, M'}(z)$ specify optically coupled Zeeman pairs. Here we introduce the reduced dynamic polarizability $\alpha = \chi^2 / \Delta$, with the Rabi frequency $\chi = -(1/2) \times \langle H \| D \| G \rangle E / \sqrt{3}$ defined in terms of the reduced dipole matrix element and the (equal) strengths of individual laser E fields.

The derived optical potentials and the corresponding dressed states depend on the adjustable detuning δ , see Fig. 1. Because of the $\delta \leftrightarrow -\delta$ mapping, for $\delta=0$ the optical potentials for the two sets of Zeeman levels coincide. However, the resulting U_+ and U_- potentials are energetically shifted with respect to each other and this energy gap might lead to a nonuniform loading of the lattice. Below we optimize the choice of the detuning δ .

First we focus on the $-3/2, +1/2$ optically coupled Zeeman pair. A particular choice of $\delta = -\alpha/15$ leads to a pair of potentials,

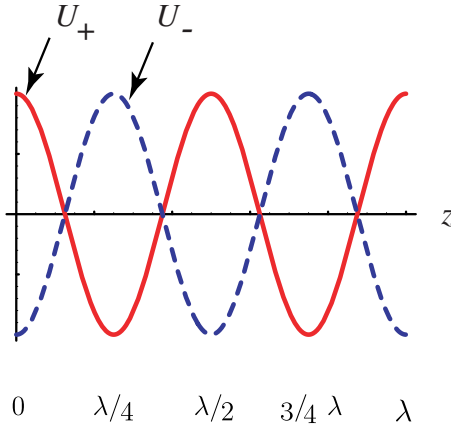


FIG. 2. (Color online) Optical potentials, Eq. (4), for the optimal choice of Raman detuning δ . While each individual potential $U_+(z)$ and $U_-(z)$ has a $\lambda/2$ periodicity, the minima of the potentials interweave, with the resulting distance between trapped atoms being $\lambda/4$.

$$U_{\pm}(z) = -\frac{\alpha}{3} \pm \frac{\alpha}{10\sqrt{3}} \cos(2kz), \quad (4)$$

that are energetically equivalent (see Fig. 2). As an additional benefit, at this value of δ the potentials have the largest intersite barriers. In going from Eq. (3) and (4), we have taken $\sqrt{\cos^2(2kz)} = \cos(2kz)$ rather than $|\cos(2kz)|$ to avoid important nonadiabatic coupling between the potentials that would occur had we taken the absolute value [6,7]. Qualitatively, the detuning $\delta = -\alpha/15$ is chosen to compensate for the difference in the light shifts for the two sublevels. As shown in Fig. 2, the minima of each individual potential are separated by $\lambda/2$. In addition, the potentials are shifted with respect to each other. This produces potential minima separated by $\lambda/4$. In other words, if the lattice is properly loaded, the distance between the neighboring atoms is $\lambda/4$. Compared to the conventional $\lambda/2$ lattices, the use of the described Raman configurations increases the atomic dipolar interactions by a factor of 2^3 . The eigenstates of the optical Hamiltonian [omitting the potential dependence, cf. Eq. (2)] are

$$\phi_{\pm}(\xi, z, t) = \frac{1}{\sqrt{2}} (|-3/2\rangle e^{-i(E_{-3/2} - \delta/2)t} \mp |+1/2\rangle e^{-i(E_{+1/2} + \delta/2)t}). \quad (5)$$

Of course, the separation between adjacent potential minima in conventional $\text{lin} \perp \text{lin}$ lattices is also $\lambda/4$, but each adjacent minima contains atoms in a given magnetic substate and is not suitable for the computing scheme described in this paper.

The problem with the above choice of detuning $\delta = -\alpha/15$ is that it optimizes only the potentials for the $-3/2, +1/2$ pair. For the other, $+3/2, -1/2$, pair the optimal choice would be $\delta' = +\alpha/15$. If we keep the $\delta = -\alpha/15$ detuning, the height of the intersite barriers for the $+3/2, -1/2$ pair would be just $\sim 20\%$ of the optimal values and in addition the corresponding $U_+(z)$ and $U_-(z)$ potentials would be energetically separated. To rectify this problem, we envi-

sion adding another independent set of four laser beams. To distinguish between the two sets, we will use primed quantities for this second set. This second quadruplet would be Raman resonant for the $+3/2, -1/2$ coupled sublevels. The required detuning is $\delta' = \alpha/15 = -\delta$. We further require that the relative phases of the laser fields for the two quads are adjusted so that both resulting sets of U_+/U_- potentials coincide, i.e., $U'_{\pm}(z) \equiv U_{\pm}(z)$. The eigenstates are

$$\phi'_{\pm}(\xi, z, t) = \frac{1}{\sqrt{2}} (|3/2\rangle e^{-i(E_{3/2} - \delta/2)t} \mp |-1/2\rangle e^{-i(E_{-1/2} + \delta/2)t}). \quad (6)$$

We assume that the dominant trapping is produced by the (two-photon) resonant fields, but detailed calculations are needed to confirm this assumption.

Notice that in the B -field gradient the Raman detuning δ would change across the lattice sites. However, the change (~ 1 kHz increment per site) is small compared to the typical light shifts, ~ 1 MHz, implying that the resonance conditions $\delta = \pm \alpha/15$ is little changed over the entire sample.

To summarize results of the discussion so far, we have designed a confinement scheme for $J=3/2$ atoms in magnetic fields. The atoms are separated by a distance of $\lambda/4$, improving the performance of multiatom gates over the conventional $\lambda/2$ schemes. In the following section we address operations of a quantum computer based on the described $\lambda/4$ lattice.

IV. OPERATION

First we define the qubit states in terms of the eigenstates, Eqs. (5) and (6), of the optical Hamiltonian. We assume that the atoms are in the Lamb-Dicke confinement regime, and the atoms are trapped at the minima of the $U_+(z)$ and $U_-(z)$ potentials (Fig. 2) with 1:1 occupation ratio. The definition of the qubit depends on whether the atom is trapped at $U_+(z)$ or $U_-(z)$ minima. For the $U_+(z)$ wells,

$$z_n^{(+)} = \frac{\lambda}{2} n, \quad |1\rangle = \phi_+, \quad |0\rangle = \phi'_+,$$

while for the $U_-(z)$ wells

$$z_n^{(-)} = \frac{\lambda}{4} + z_n^{(+)}, \quad |1\rangle = \phi_-, \quad |0\rangle = \phi'_-,$$

where n is an integer. To individually address the qubits, we introduce a B -field gradient and use pulses of microwave radiation of various duration to execute one-qubit operations. However, compared to Ref. [1], here we deal with the dressed states. Describing dynamics of the system requires certain care. For concreteness, we focus on an atom in the U_+ well, but the conclusions will apply equally to the U_- wells. The total Hamiltonian including interaction V_M with circularly polarized MW radiation of frequency ω reads $H = H_{\text{opt}} + V_M e^{-i\omega t} + V_M^\dagger e^{+i\omega t}$. The duration of the drive should be chosen to resolve different Zeeman transition frequencies between ground state sublevels near the potential minima of a single well, as well as transition frequencies between adja-

cent U_+ and U_- potential wells. These conditions can be satisfied easily, as the change of the Zeeman frequency for two neighboring sites is ~ 1 kHz, while the light shifts are in the order of 1 MHz. Under such an assumption, the atomic wave function can be expanded as $\Psi(t) = c(t)\tilde{\phi}_+ + c'(t)\tilde{\phi}'_+$. Taking into account Eq. (1), we arrive at the system of coupled equations for the expansion amplitudes,

$$i\dot{c} = \langle \phi_+ | V_M e^{-i\omega t} + V_M^\dagger e^{+i\omega t} | \phi'_+ \rangle c'(t),$$

$$i\dot{c}' = \langle \phi'_+ | V_M e^{-i\omega t} + V_M^\dagger e^{+i\omega t} | \phi_+ \rangle c(t).$$

While evaluating matrix elements we find that the resonant frequencies are $\omega_{\text{res}} = \omega_Z, \omega_Z \pm \delta$, where $\omega_Z = \frac{4}{3}\mu_B B_0$. The resonance at ω_Z corresponds to transitions between the $M = -1/2$ and $M = 1/2$ sublevels, while those at $\omega_Z \pm \delta$ correspond to transitions between $M = -3/2$ and $M = -1/2$ or $M = 1/2$ and $M = 3/2$. Again, due to the orders-of-magnitude difference in the Zeeman and the light-shift energy scales, we may resolve these resonance frequencies and find it convenient to work at ω_Z . For the selected transition, the above system of equations maps onto the problem of a two-level system in an oscillating field. By varying the duration of the MW pulses, we may execute arbitrary rotations in the Hilbert space spanned by individual qubits.

Since the Zeeman splitting is position dependent, only a single qubit from the entire ensemble will respond to a pulse of a certain frequency. The advantage of the proposed addressing scheme is that there is no need to focus radiation on an individual atom.

Now we turn to another important ingredient of Quantum Computer architectures: multiqubit gates. It is sufficient to consider operation of the universal two-qubit CNOT gate [9]. In the proposal of Ref. [9] the resonance frequency of the target qubit should depend on the state of the control qubit. This leads to a conditional quantum dynamics: the transition in the target qubit occurs only if the control qubit is in a predefined state. In our scheme, this dependence of the resonance frequency is due to magnetic interactions between two neighboring atoms. Indeed, we find that each qubit state possesses a permanent magnetic-dipole moment aligned with the z axis: $\mu_{|1\rangle} = +2/3\mu_B$, $\mu_{|0\rangle} = -2/3\mu_B$ (these values are independent of the well). The generated magnetic field at the position of the target qubit is $\delta B = 2\alpha^2/R^3\mu_{|1,0\rangle}$, where $\alpha \approx 1/137$ is the fine-structure constant and $R = \lambda/4$ is the distance between the qubits. Depending on the state of the control qubit the generated field will either increase or reduce the offset B field $B_0(z)$ and modify the Zeeman frequency. While performing the gate, one needs to resolve the frequency difference

$$\delta\omega_{\text{CNOT}} = \frac{32}{9}\alpha^2\frac{\mu_B^2}{R^3}.$$

The minimum duration of the MW pulse is $\tau_{\text{CNOT}} \sim 1/\delta\omega_{\text{CNOT}}$. For our parameters, $\tau_{\text{CNOT}} \approx 10^{-3}$ s. The resulting performance is competitive with other quantum computing schemes such as nuclear magnetic resonance [10] ($\tau_{\text{CNOT}} \sim 10^{-3} - 10^{-2}$ s), and controlled collisions [11] ($\tau_{\text{CNOT}} \sim 4 \times 10^{-4}$ s).

V. MOTIONAL AND MAGNETIC-NOISE INDUCED DECOHERENCES

The gate operations must be much faster than decoherence rates. A number of decoherence mechanisms present in the current proposal have been analyzed in Ref. [1]. For example, atoms may be lost due to an entanglement of the internal and motional degrees of freedom during the NOT-gate operation. It was demonstrated [1] that the associated excitation rates from the ground motional state are negligible. The underlying reason is that the induced perturbation is adiabatically slow: on the time scale of the NOT pulse, the atomic c.m. undergoes many oscillations in the well. The same conclusion holds for the present proposal. However, the dressed (qubit) states were introduced in Sec. III neglecting the c.m. motion and we need to additionally consider coupling of dressed states due to the atomic motion. Fortunately, as shown below, it is straightforward to demonstrate that the qubit states are not coupled by the c.m. motion.

Another important source of the decoherence arises due to magnetic noise. The qubit states are defined in terms of the Zeeman sublevels sensitive to magnetic perturbations. In Ref. [1], a noise-induced dephasing has been evaluated, and it has been shown that the decoherence rate can be reduced with modest B -field shielding requirements. In the present proposal, the implications of the magnetic noise can be more severe: for dressed states, the relative phase (determined by the Zeeman splitting) between the ‘‘bare’’ magnetic substates must remain fixed. The noise perturbs the relative phase leading to excitations of the motional quanta.

In Sec. III, the dressed states $\tilde{\phi}_\pm(\xi, z, t)$ were found by assuming that the atom was localized at the position z and then by diagonalizing the position-dependent optical matrix $W(z)$. Taking into account that for a fixed z , the $\tilde{\phi}_\pm(\xi, z, t)$ form a complete basis set, we may expand the exact wave function as

$$\Psi(\xi, z, t) = \chi_-(z, t)\tilde{\phi}_-(\xi, z, t) + \chi_+(z, t)\tilde{\phi}_+(\xi, z, t), \quad (7)$$

where $\chi_\pm(z)$ are (generally coupled) c.m. wave functions of interest. The Hamiltonian including the c.m. motion is

$$H(\xi, z, t) = T + H_{\text{opt}}(\xi, z, t), \quad (8)$$

with $T = -\frac{1}{2M}\frac{\partial^2}{\partial z^2}$ being the kinetic energy operator for the c.m. motion. Using the standard technique of projecting the Schrödinger equation onto the $\tilde{\phi}_\pm$ basis, we find

$$i\frac{\partial}{\partial t}\chi_\pm(z, t) = \sum_{p=\pm} \langle \phi_\pm | T | \phi_p \chi_p \rangle_\xi + U_\pm(z)\chi_\pm(z, t), \quad (9)$$

where the inner product is with respect to the internal degrees of freedom ξ . The coupling between the two components χ_+ and χ_- arises in general due to the off-diagonal term in the sum. In our case, the dressed states $\phi_\pm(\xi, t)$ do not depend on z , Eqs. (5) and (6), and we arrive at a simple result

$$i\frac{\partial}{\partial t}\chi_{\pm}(z,t) = -\frac{1}{2M}\frac{\partial^2}{\partial z^2}\chi_{\pm}(z,t) + U_{\pm}(z)\chi_{\pm}(z,t). \quad (10)$$

This is a physically significant result: the atomic motion does not lead to mixing of the qubit states.

At the minima of the potentials, the bottom of the potential well can be approximated by a harmonic oscillator potential and we can write $\chi_{\pm}(z,t)$ as a sum of the time-dependent stationary states of the harmonic oscillator χ_n ,

$$\chi_{\pm}(z,t) = \sum_n c_{\pm,n}(t)\chi_n(z,t). \quad (11)$$

The coefficients $c_{\pm,n}$ depend on the temperature of the qubit and the loading process; we assume that initially only the ground motional states are occupied. We also require that the potential is sufficiently deep so that the atoms do not tunnel away, see Ref. [1] for estimates.

Now we can analyze the effect of time-dependent magnetic noise $B(t)$ acting on the qubit. Let us take, for example, the qubit in the state ϕ_+ localized in the motional ground state χ_0 of one of the minima of U_+ for $t < 0$. For $t \geq 0$, the magnetic noise is turned on and we look at the decoherence rate of the qubit. We consider the loss mechanism as a two-step process. The magnetic field acts only on the internal degree of freedom of the qubit causing a primary transition $c_{+,0}\phi_+\chi_0(z) \rightarrow c_{-,0}\phi_-\chi_0(z)$. Minima of $U_+(z)$ correspond to maxima of $U_-(z)$ so the new state $\phi_-\chi_0(z)$ is motionally unstable. For example, one of the possible transitions this state undergoes is $c_{-,0}\phi_-\chi_0(z) \rightarrow c_{-,2}\phi_-\chi_2(z)$. The exact details of this secondary transition are not important, since the entire decoherence rate is determined by the rate of the primary excitation. For example, characteristic time associated with the $c_{-,0}\phi_-\chi_0(z) \rightarrow c_{-,2}\phi_-\chi_2(z)$ route is $\tau_2 = \frac{1}{2k}\sqrt{\frac{5\sqrt{3}M}{\alpha}}$. Our estimate for Al atom, $\lambda = 309$ nm and $\alpha \sim 10^7$ Hz results in $\tau_2 \sim 10^{-7}$ s.

The decoherence rate is determined by the primary excitation $c_{+,0}\phi_+\chi_0 \rightarrow c_{-,0}\phi_-\chi_0$ and below we determine the probability associated with this process. The required time evolution of the coefficient $c_{-,0}(t)$ is computed by including the magnetic noise perturbation $\mu B(t)|\phi_-\rangle\langle\phi_+| + \text{H.c.}$ in the Schrödinger equation

$$i\frac{\partial}{\partial t}c_{-,0}(t) = (U_{\max} - U_{\min})c_{-,0}(t) + \mu B(t)c_{+,0}(t), \quad (12)$$

where $\mu = \langle\phi_-|\hat{\mu}_B^{\mathbf{B}}|\phi_+\rangle$, and $U_{\max} - U_{\min} = \frac{\alpha}{5\sqrt{3}}$ is the energy difference between the minimum and the maximum of the U_+ and U_- potentials, Eq. (4). The solution of Eq. (12) is

$$c_{-,0}(t) = -ie^{-i(\alpha/5\sqrt{3})t} \int_0^t \mu B(t_1)c_{+,0}(t_1)e^{i(\alpha/5\sqrt{3})t_1} dt_1. \quad (13)$$

The magnetic noise is characterized by its autocorrelation function

$$\langle B(t_1)B^*(t_1 + \tau) \rangle = \frac{1}{2\pi} \int_{-\infty}^{+\infty} S(\omega)e^{i\omega\tau} d\tau, \quad (14)$$

where $S(\omega)$ is the frequency-dependent spectral density of the noise. The autocorrelation function $\langle c_{-,0}(t)c_{-,0}(t) \rangle$ repre-

sents the probability $p(t)$ of excitation $\phi_+\chi_0 \rightarrow \phi_-\chi_0$,

$$p(t) = \int_0^t \int_0^t dt_1 dt_2 \mu^2 \langle B(t_1)c_{+,0}(t_1) \times B^*(t_2)c_{+,0}^*(t_2)e^{i(\alpha/5\sqrt{3})(t_1-t_2)} \rangle. \quad (15)$$

For time t sufficiently short to guarantee that $|c_{-,0}(t)| \ll |c_{+,0}(t)|$, but longer than the correlation time of the magnetic noise, we may approximate $c_{+,0}(t) \approx 1$, and find

$$p(t) = \mu^2 \int_0^t S\left(-\frac{\alpha}{5\sqrt{3}}\right) dt = \frac{1}{\tau_1} t, \quad (16)$$

with $\tau_1 = \frac{1}{\mu^2} S\left(\frac{\alpha}{5\sqrt{3}}\right)^{-1}$.

For coherence times on the order of 10 seconds the magnetic noise should satisfy

$$\sqrt{S\left(\frac{\alpha}{5\sqrt{3}}\right)} \ll 3 \times 10^{-12} \text{ T}/\sqrt{\text{Hz}}. \quad (17)$$

This level can be attained with passive shielding [12]. Moreover, notice that the spectral density of the noise is evaluated at a relatively high (~ 1 MHz) frequency. This frequency is of the order of the light shift induced by the lattice lasers. At such a high frequency the magnetic noise is highly suppressed. For example, for passive shielding, the characteristic cutoff frequency due to induced currents is in the order of kHz [12].

To conclude, our analysis suggests that magnetic noise can be controlled at an adequate level. Also the atomic motion does not lead to entanglement of qubit states, defined as dressed atomic Zeeman sublevels. Other sources of decoherence common with the present proposal, were considered in Ref. [1] and we refer the reader to that paper for details.

VI. CONCLUSION

We have outlined a method for increasing the relatively weak magnetic interactions in which atoms are trapped in Raman optical lattices having reduced periodicity. The reduced interatomic distances lead to improved performance of multiqubit gates. In the particular case of the Al, $J=3/2$ Zeeman manifold, we designed a $\lambda/4$ optical lattice and found that universal two-qubit CNOT-gate operations require times of approximately 10^{-3} s. These times are comparable to other quantum computing schemes such as nuclear magnetic resonance [10] and controlled collisions [11]. Moreover, the present proposal offers scalability, individual qubit addressability with *unfocused* beams of microwave radiation, and coherent “always-on” interactions between the qubits.

Analysis of Refs. [2,3] suggests that in general, the standing-wave Raman fields should lead to $\lambda/2^n$ ($n=1,2,3,\dots$) interatomic separations. For a given number of atoms, such lattices should improve performance of the original $\lambda/2$ quantum computing architecture of Ref. [1] by an exponentially increasing factor of $2^{3(n-1)}$. It remains to be seen if the present $\lambda/4$ proposal can be generalized to optical lattices of smaller periodicity.

ACKNOWLEDGMENTS

The authors would like to thank D. Budker and D. DeMille for discussions. One of the authors (A.D.) would like to thank for the hospitality the FOCUS center, where a

part of this work has been completed. This work was supported in part by the NSF Grants Nos. PHY-0354876, PHY0244841, the NSF FOCUS Center Grant, and the Michigan Center for Theoretical Physics.

-
- [1] A. Derevianko and C. C. Cannon, Phys. Rev. A **70**, 062319 (2004).
- [2] B. Dubetsky and P. R. Berman, Phys. Rev. A **66**, 045402 (2002).
- [3] B. Dubetsky and P. R. Berman, Laser Phys. **12**, 1161 (2002).
- [4] R. Zhang, N. V. Morrow, P. R. Berman, and G. Raithel, Phys. Rev. A **72**, 043409 (2005).
- [5] D. Jaksch, J. I. Cirac, P. Zoller, S. L. Rolston, R. Cote, and M. D. Lukin, Phys. Rev. Lett. **85**, 2208 (2000).
- [6] V. S. Malinovsky and P. R. Berman, Opt. Commun. (to be published).
- [7] P. R. Berman, G. Raithel, R. Zhang, and V. S. Malinovsky, Phys. Rev. A **72**, 033415 (2005).
- [8] R. W. McGowan, D. M. Giltner, and S. A. Lee, Opt. Lett. **20**, 2535 (1995).
- [9] A. Barenco, D. Deutsch, A. Ekert, and R. Jozsa, Phys. Rev. Lett. **74**, 4083 (1995).
- [10] R. Laflamme *et al.*, e-print quant-ph/0207172.
- [11] T. Calarco, E. A. Hinds, D. Jaksch, J. Schmiedmayer, J. I. Cirac, and P. Zoller, Phys. Rev. A **61**, 022304 (2000).
- [12] D. Budker, D. F. Kimball, and D. P. DeMille, *Atomic Physics: Exploration Through Problems and Solutions*, 1st ed. (Oxford University Press, Oxford, 2003).